

## Drift-tearing magnetic islands in tokamak plasmas

R. Fitzpatrick and F. L. Waelbroeck

*Institute for Fusion Studies, Department of Physics, University of Texas at Austin, Austin, Texas 78712, USA*

(Received 30 October 2007; accepted 5 December 2007; published online 23 January 2008)

A systematic fluid theory of nonlinear magnetic island dynamics in conventional low- $\beta$ , large aspect-ratio, circular cross-section tokamak plasmas is developed using an extended magnetohydrodynamics model that incorporates diamagnetic flows, ion gyroviscosity, fast parallel electron heat transport, the ion sound wave, the drift wave, and average magnetic field-line curvature. The model excludes the compressible Alfvén wave, geodesic field-line curvature, neoclassical effects, and ion Landau damping. A collisional closure is used for plasma dynamics parallel to the magnetic field. Two distinct branches of island solutions are found, namely the “sonic” and “hypersonic” branches. Both branches are investigated analytically, using suitable ordering schemes, and in each case the problem is reduced to a relatively simple set of nonlinear differential equations that can be solved numerically via iteration. The solution determines the island phase velocity, relative to the plasma, and the effect of local currents on the island stability. *Sonic* islands are relatively wide, flatten both the temperature and density profiles, and tend to propagate close to the local ion fluid velocity. *Hypersonic* islands, on the other hand, are relatively narrow, only flatten the temperature profile, radiate drift-acoustic waves, and tend to propagate close to the local electron fluid velocity. The hypersonic solution branch ceases to exist above a critical island width. Under normal circumstances, both types of island are *stabilized* by local ion polarization currents. © 2008 American Institute of Physics. [DOI: 10.1063/1.2829757]

### I. INTRODUCTION

A magnetic confinement device is designed to trap a thermonuclear plasma on a set of toroidally nested magnetic flux-surfaces.<sup>1</sup> Heat and particles *flow around* flux-surfaces relatively rapidly due to the free streaming of charged particles along magnetic field-lines. On the other hand, heat and particles are only able to *diffuse across* flux-surfaces relatively slowly, assuming that the magnetic field-strength is sufficiently large to render the particle gyroradii much smaller than the minor radius of the device. This article will concentrate on *tokamaks*, which are a type of *toroidally axisymmetric* magnetic confinement device in which the magnetic field is dominated by an approximately uniform toroidal component whose energy density is much larger than that of the plasma.<sup>2</sup>

Tokamak plasmas are subject to a number of macroscopic instabilities that limit their effectiveness.<sup>2</sup> Such instabilities can be divided into two broad classes. So-called *ideal instabilities* are nonreconnecting modes that destroy the plasma in a matter of microseconds. However, such instabilities can easily be avoided by limiting the plasma pressure and/or by tailoring the magnetic equilibrium.<sup>3</sup> *Tearing modes*, on the other hand, are relatively slowly growing instabilities that are far more difficult to avoid.<sup>3,4</sup> These instabilities tend to saturate at relatively low levels,<sup>5–7</sup> in the process reconnecting magnetic flux-surfaces to form helical structures known as *magnetic islands*. Magnetic islands are radially localized structures centered on so-called *rational flux-surfaces*, which satisfy  $\mathbf{k} \cdot \mathbf{B} = 0$ , where  $\mathbf{k}$  is the wave number of the instability, and  $\mathbf{B}$  is the equilibrium magnetic field. Magnetic islands degrade plasma confinement because

they enable heat and particles to flow very rapidly along field-lines from their inner to their outer radii, implying an almost complete loss of confinement in the region lying between these radii.<sup>8</sup>

The aim of this paper is to develop a systematic fluid theory of tearing mode dynamics in conventional low- $\beta$ , large aspect-ratio, circular cross-section tokamak plasmas. For the sake of simplicity, we shall use a slab approximation to model the magnetic geometry, and employ a collisional closure for the plasma dynamics parallel to the magnetic field. Magnetic islands that are sufficiently wide to significantly degrade overall energy confinement are, in effect, helical magnetic equilibria. Moreover, the equations governing such equilibria are nonlinear in nature.<sup>2</sup> Hence, our investigation will concentrate on *nonlinear* tearing mode dynamics.

Given that tearing modes are *macroscopic* instabilities, it is natural to investigate them using some form of *fluid* model. Unfortunately, while the well-known, and relatively simple, magnetohydrodynamic (MHD) model is appropriate for describing violently unstable plasma instabilities, it fails to capture many important aspects of slowly evolving instabilities such as tearing modes.<sup>9</sup> Consequently, it is necessary to use some form of *extended-MHD* model in our investigation. The particular model employed in this paper is the so-called *five-field model*,<sup>10–12</sup> which is a generalization of the well-known *four-field model* of Hazeltine *et al.*<sup>13</sup> The five-field model is derived using a low- $\beta$ , drift-MHD ordering of plasma parameters.<sup>9</sup> It incorporates diamagnetic flows, ion gyroviscosity, fast parallel electron heat transport, the shear-Alfvén wave, the ion sound wave, the drift wave, and average magnetic field-line curvature. However, the compres-

sional Alfvén wave, which propagates much faster than the aforementioned waves in a low- $\beta$  plasma, effectively decoupling from them, is excluded from the model. (Incidentally, a tearing mode is a modified shear-Alfvén wave.) Electron inertia is also neglected in the model, since it has a negligible effect on slowly evolving instabilities. The main failings of the five-field model are that it uses a collisional closure for plasma dynamics parallel to the magnetic field, and that it neglects ion Landau damping.

For those interested, Ref. 14 includes a comprehensive history and discussion of previously published fluid theories of magnetic islands in tokamaks.

## II. PRELIMINARY ANALYSIS

### A. Coordinates

For the sake of simplicity, let us work in slab geometry, using the associated right-handed Cartesian coordinates  $(x, y, z)$ . Suppose that there is no variation of quantities in the  $z$  direction, i.e.,  $\partial/\partial z \equiv 0$ . The system is assumed to be periodic in the  $y$  direction, with periodicity length  $2\pi/k$ . Roughly speaking, the  $x$  direction represents the radial direction, the  $y$  direction the poloidal direction, and the  $z$  direction the direction along the resonant field-line.

### B. Asymptotic matching

Consider a quasineutral plasma consisting of electrons and singly charged ions. The plasma is conveniently divided into an “inner region,” which comprises the plasma in the immediate vicinity of the island, and an “outer region,” which comprises the remainder of the plasma. As is well known, the five-field equations reduce to the much simpler *ideal-MHD* equations in the outer region.<sup>4</sup> Let us assume that a conventional ideal-MHD solution has been found in this region. The solution is characterized by a single parameter,  $\Delta'$ , defined as the jump in the logarithmic derivative of the  $x$  component of the perturbed magnetic field across the inner region.<sup>4</sup> This parameter measures the free energy available in the outer region to drive the tearing mode. The mode is destabilized if  $\Delta' > 0$ . It, therefore, remains to solve the five-field equations in the inner region, and then to asymptotically match this solution to the previously obtained ideal-MHD solution at the boundary between the inner and outer regions.

### C. Plasma equilibrium

The plasma equilibrium is assumed not to vary in the  $y$  direction. The inner region is confined to a relatively thin layer, centered on the rational surface. In this region, the equilibrium magnetic field takes the form

$$\mathbf{B} = B_z \left( \frac{x}{L_s} \mathbf{e}_y + \mathbf{e}_z \right), \quad (1)$$

where  $B_z$  is a uniform constant, and  $L_s$  is the *magnetic shear length*. Likewise, the equilibrium electron number density is written

$$n_e = n_{e0} \left( 1 + \frac{x}{L_n} \right), \quad (2)$$

where  $n_{e0}$  is a uniform constant and  $L_n$  is the *density gradient scale-length*. The equilibrium electron temperature takes the form

$$T_e = T_{e0} \left( 1 + \frac{x}{L_T} \right), \quad (3)$$

where  $T_{e0}$  is a uniform constant and  $L_T$  is the *electron temperature gradient scale-length*. For the sake of simplicity, the ion temperature is assumed to take the constant value  $T_i$ . Furthermore, the equilibrium  $\mathbf{E} \times \mathbf{B}$  velocity is assumed to be uniform. Finally, the plasma is subject to a uniform gravitational acceleration  $g$  in the  $-x$  direction. This acceleration is intended to mimic the effect of *average magnetic field-line curvature*.<sup>15</sup> In fact, the effective radius of curvature of the field-lines is given by  $L_c = (T_{e0} + T_i)/m_i g$ , where  $m_i$  is the ion mass.

### D. Tearing perturbation

Suppose that the plasma equilibrium is perturbed by a tearing instability that is periodic in the  $y$  direction with wave number  $k$ . Note that  $\mathbf{k} \cdot \mathbf{B} = 0$  at  $x=0$ . Hence, the rational surface lies at  $x=0$ . The instability is assumed to saturate at a relatively low amplitude to produce a thin (relative to the width of the plasma in the  $x$  direction) magnetic island. The magnetic island is wholly contained within the inner region. Let the width of the island in the  $x$  direction satisfy

$$w \ll L_s, L_n, L_T, L_c, k^{-1}. \quad (4)$$

Finally, suppose that the island propagates in the  $y$  direction at some steady phase-velocity  $V_p$ .

### E. Important plasma parameters

At this stage, it is helpful to define the following important plasma parameters. First, the *electron beta*,

$$\beta = \frac{\mu_0 n_{e0} T_{e0}}{B_z^2}, \quad (5)$$

which is assumed to be much less than unity. Second, the *ion sound radius*,

$$\rho_s = \frac{\sqrt{T_{e0}/m_i}}{(eB_z/m_i)}, \quad (6)$$

which is assumed to be less than, or of order, the width of the inner region, and, therefore, much smaller than  $L_s, L_n, L_T, L_c$ , or  $k^{-1}$ . Here,  $e$  is the magnitude of the electron charge. Third, the *electron diamagnetic velocity*,

$$V_* = \frac{T_{e0}}{eB_z L_n}. \quad (7)$$

The island phase-velocity is assumed to be of order  $V_*$ . Fourth, the *shear parameter*,

$$\epsilon_n = \frac{L_n}{L_s}, \quad (8)$$

which is assumed to be much less than unity. Fifth, the *ion to electron temperature ratio*,

$$\tau = \frac{T_i}{T_{e0}}, \quad (9)$$

which is assumed to be less than or of order unity. Finally, the *curvature parameter*,

$$\gamma_c = \frac{2L_s^2}{L_c L_n}, \quad (10)$$

which is also assumed to be less than or of order unity. Note that  $\gamma_c > 0$  corresponds to *unfavorable* average magnetic field-line curvature.<sup>15</sup>

It is also helpful to define the normalized beta,

$$\hat{\beta} = \frac{\beta}{\epsilon_n}, \quad (11)$$

the normalized ion sound radius,

$$\rho = \frac{\rho_s}{w}, \quad (12)$$

and the *ion sound parameter*,

$$\alpha = \sqrt{1 + \tau} \frac{\epsilon_n}{\rho}. \quad (13)$$

This last parameter measures how effective ion sound waves are at flattening the plasma density across the island (they are effective if  $\alpha \gg 1$ , and ineffective if  $\alpha \ll 1$ ).

## F. Five-field model

According to the five-field model,<sup>10-12</sup> a *steady-state* inner region solution in the *island rest frame* is governed by the following set of equations:

$$0 = [\phi - n - \zeta T, \psi] + \rho^4 C J, \quad (14)$$

$$0 = [\phi, n] + [V + \rho^2 J, \psi] - \rho^2 \alpha^2 (1 + \tau)^{-1} \gamma_c [x, \phi - n] + \rho^2 D n_{xx}, \quad (15)$$

$$0 = [\phi, \phi_{xx}] + [J, \psi] + \alpha^2 \gamma_c [x, n] - \frac{\tau}{2} \{ [\phi_{xx}, n] + [n_{xx}, \phi] + [\phi, n]_{xx} \} + \rho^2 \mu (\phi + \pi)_{xxxx}, \quad (16)$$

$$0 = [\phi, V] + \alpha^2 [n + T/(1 + \tau), \psi] + \rho^2 \chi V_{xx}, \quad (17)$$

$$0 = \rho^{-2} \kappa_{\parallel} [[T, \psi], \psi] + (3/2) [\phi, T] + [V + \zeta \rho^2 J, \psi] + \rho^2 \kappa_{\perp} T_{xx}, \quad (18)$$

with all lengths normalized to  $w$  and all velocities to  $V_*$ . Here,  $w$  is one-quarter of the constant- $\psi$  magnetic island width in the  $x$  direction. The first equation is the generalized Ohm's law, the second ensures fluid continuity, the third is the parallel ion vorticity equation, the fourth determines parallel ion flow, and the fifth governs electron heat flow. Also,  $\zeta = 1.71$ ,

$$\psi_{xx} = -1 + \hat{\beta} \rho^2 J, \quad (19)$$

and

$$[A, B] \equiv A_x B_{\theta} - A_{\theta} B_x, \quad (20)$$

where  $\theta = ky$ . In the above equations,  $\psi = A_z L_s / (B_z w^2)$ ,  $J = (1 - \mu_0 j_z L_s / B_z) / (\hat{\beta} \rho^2)$ ,  $\phi = -\Phi / (B_z w V_*)$ ,  $n = -(L_n / w)(n_e - n_{e0}) / n_{e0}$ ,  $T = -(L_n / w)(T_e - T_{e0}) / T_{e0}$ ,  $V = (L_n / L_s) V_{zi} / V_*$ ,  $\eta = (\eta_{\parallel} / \mu_0) / (k V_* \rho_s^2)$ ,  $C = \hat{\beta} \eta$ ,  $\kappa_{\parallel} = (k \rho_s)^2 (\kappa_{\parallel e} / n_{e0}) / (k V_* L_s^2)$ ,  $\mu = (\mu_{\perp i} / n_{e0} m_i) / (k V_* \rho_s^2)$ ,  $\kappa_{\perp} = (\kappa_{\perp e} / n_{e0}) / (k V_* \rho_s^2)$ ,  $D = \beta \eta + \kappa_{\perp}$ ,<sup>16</sup> and  $\chi = 4\mu$ .<sup>11</sup> Moreover,  $A_z$  is the  $z$  component of the magnetic vector potential,  $j_z$  is the  $z$  component of the electric current density,  $\Phi$  is the electric scalar potential,  $V_{zi}$  is the  $z$  component of the ion fluid velocity,  $\eta_{\parallel}$  is the parallel (to the magnetic field) plasma resistivity,  $\mu_{\perp i}$  is the perpendicular ion viscosity,  $\kappa_{\parallel e}$  is the parallel electron heat conductivity, and  $\kappa_{\perp e}$  is the perpendicular electron heat conductivity. The various transport parameters are all assumed to be uniform constants. Note that  $\psi(x, \theta)$  is a magnetic flux-function,  $\phi(x, \theta) + \pi n(x, \theta)$  is an ion fluid stream-function, and  $\phi(x, \theta) - n(x, \theta)$  is an electron fluid stream-function.

Our system is periodic in the  $\theta$  direction with period  $2\pi$ . For the case of a tearing mode, we expect  $\psi, J, V$  to be even in  $x$ , and  $\phi, n, T$  to be odd.<sup>4</sup> The boundary conditions at the edge of the inner region are

$$\psi \rightarrow -x^2/2 + \cos \theta, \quad (21)$$

$$n_x \rightarrow -1, \quad (22)$$

$$T_x \rightarrow -\eta_e, \quad (23)$$

$$\phi_x \rightarrow \left( \frac{V_p - V_{EB}}{V_*} \right), \quad (24)$$

$$\phi_{xxx}, J, V \rightarrow 0, \quad (25)$$

as  $|x| \rightarrow 0$ . Here,  $V_p$  is the island phase-velocity,  $V_{EB}$  is the equilibrium  $\mathbf{E} \times \mathbf{B}$  velocity (both in the  $y$  direction), and  $\eta_e = L_n / L_T$ .

Finally, asymptotic matching between the solutions in the inner and outer regions yields the well-known relation<sup>5</sup>

$$3.29 \eta^{-1} \frac{d(w/\rho_s)}{dt} = \Delta' \rho_s - 4 \hat{\beta} \rho^3 \int_0^{\infty} \oint J \cos \theta \frac{d\theta}{2\pi} dx, \quad (26)$$

where  $\Delta'$  is the tearing stability index.<sup>4</sup> The first and second terms on the right-hand side of the above equation parametrize the contributions to the free energy available to drive the tearing mode which originate from the outer and the inner regions, respectively. Note that the magnetic island grows and decays on the very slow *resistive* time scale,  $\eta^{-1}$ .

## G. Constant- $\psi$ approximation

Suppose that

$$\hat{\beta} \rho^2 \ll 1. \quad (27)$$

It follows from Eqs. (19) and (21) and the easily verified fact that  $|J| \leq O(1)$  that

$$\psi(x, \theta) \simeq -x^2/2 + \cos \theta. \quad (28)$$

The above magnetic flux-function maps out a magnetic island, centered on  $x=0$ . The O-point lies at  $x=0$  and  $\theta=0$ , whereas the X-point lies at  $x=0$  and  $\theta=\pi$ . The magnetic separatrix corresponds to  $\psi=-1$ . Finally, the full width of the separatrix in the  $x$  direction is 4. Hence, the unnormalized full island width is  $4w$ .

### H. Flux-surface average operator

The *flux-surface average operator* is defined as the annihilator of  $[A, \psi]$  for any  $A(x, \theta)$ , i.e.,

$$\langle [A, \psi] \rangle \equiv 0. \quad (29)$$

It is easily show, from Eq. (28), that

$$\langle f(\psi, \theta) \rangle = \oint \frac{f(\psi, \theta) d\theta}{|x| 2\pi} \quad (30)$$

outside the magnetic separatrix, and

$$\langle f(s, \psi, \theta) \rangle = \int_{-\theta_0}^{\theta_0} \frac{f(s, \psi, \theta) + f(-s, \psi, \theta) d\theta}{2|x| 2\pi} \quad (31)$$

inside the separatrix, where  $s=\text{sgn}(x)$  and  $x(s, \psi, \theta_0)=0$ . Here, the  $\theta$  integrals are carried out at constant  $\psi$ . Incidentally, Eq. (26) can be written

$$\frac{dw}{dt} \propto \Delta' \rho_s + 4\hat{\beta}\rho^3 \int_1^{-\infty} \langle J \cos \theta \rangle d\psi. \quad (32)$$

### I. Primary ordering scheme

Our primary ordering scheme depends on the fact that the hot plasmas found in modern-day tokamaks are characterized by very *fast* [compared to  $(kV^*)^{-1}$ ] transport of heat *along* magnetic field-lines, and very *slow* diffusion of magnetic flux, particles, momentum, and heat *across* magnetic flux-surfaces, i.e.,

$$\kappa_{\parallel} \gg 1 \gg C, D, \mu, \chi, \kappa_{\perp}. \quad (33)$$

All other quantities in our model are assumed to be  $O(1)$  by comparison with  $\kappa_{\parallel}$ ,  $C$ ,  $D$ ,  $\mu$ ,  $\chi$ , and  $\kappa_{\perp}$ . Let  $O(1)$  quantities be denoted *zeroth-order*, while quantities that are  $O(C)$  are first-order, etc. (This ordering is sometimes referred to as the *transport ordering*.<sup>9,19</sup>) The five fields in our model ( $\phi$ ,  $J$ ,  $n$ ,  $V$ , and  $T$ ) are all expanded in the form

$$\phi = \phi^{(0)} + \phi^{(1)} + \phi^{(2)}, \quad (34)$$

etc., where  $\phi^{(n)}$  is  $n$ th order.

### J. Secondary ordering scheme

Our secondary ordering scheme depends on the inequality

$$\epsilon_n \ll 1, \quad (35)$$

which holds in conventional tokamak discharges (since  $L_n$  is generally of order the minor radius of the device, whereas  $L_s$  is of order the major radius, and the major radius is much larger than the minor radius in a conventional tokamak). This

inequality allows us to distinguish between two different island regimes. In the *sonic* regime,

$$w \sim \frac{\rho_s}{\epsilon_n}, \quad (36)$$

which implies that  $\alpha \sim 1$  and  $\rho \sim \epsilon_n \ll 1$ . On the other hand, in the *hypersonic* regime,

$$w \sim \rho_s, \quad (37)$$

which implies that  $\rho \sim 1$  and  $\alpha \sim \epsilon_n \ll 1$ . The main physical distinction between the sonic and hypersonic regimes is that ion sound waves are able to propagate around island flux-surfaces sufficiently rapidly to flatten the density profile within the magnetic separatrix in the former regime, but not in the latter.<sup>17</sup> It is convenient to subdivide the sonic regime into the *subsonic* regime, characterized by  $\alpha \gg 1$ ; the true *sonic* regime, characterized by  $\alpha \sim 1$ ; and the *supersonic* regime, characterized by  $\epsilon_n \ll \alpha \ll 1$ . In the following, it is assumed that  $\tau$ ,  $\eta_e$ , and  $\gamma_c$  are all  $O(1)$ .

## III. SONIC ISLANDS

### A. Introduction

As we have just mentioned, sonic islands are characterized by the secondary ordering  $\rho \ll 1$  and  $\alpha \sim O(1)$ .

### B. Zeroth-order terms

Retaining only zeroth-order terms in our primary ordering scheme, the five-field equations reduce to

$$0 = [\phi^{(0)} - n^{(0)} - \zeta T^{(0)}, \psi], \quad (38)$$

$$0 = [\phi^{(0)}, n^{(0)}] + [V^{(0)} + \rho^2 J^{(0)}, \psi] - \rho^2 \alpha^2 (1 + \tau)^{-1} \gamma_c [x, \phi^{(0)} - n^{(0)}], \quad (39)$$

$$0 = [\phi^{(0)}, \phi_{xx}^{(0)}] + [J^{(0)}, \psi] + \alpha^2 \gamma_c [x, n^{(0)}] - \frac{\tau}{2} \{ [\phi_{xx}^{(0)}, n^{(0)}] + [n_{xx}^{(0)}, \phi^{(0)}] + [\phi^{(0)}, n^{(0)}]_{xx} \}, \quad (40)$$

$$0 = [\phi^{(0)}, V^{(0)}] + \alpha^2 [n^{(0)} + T^{(0)}/(1 + \tau), \psi], \quad (41)$$

$$0 = [[T^{(0)}, \psi], \psi]. \quad (42)$$

It immediately follows from Eq. (42) that

$$T^{(0)} = T(\psi). \quad (43)$$

In other words, the lowest-order electron temperature profile is a *flux-surface function*. Since  $T$  is odd in  $x$ , whereas  $\psi$  is even, it follows that  $T=0$  inside the magnetic separatrix. Hence, the electron temperature profile is *flattened* within the magnetic separatrix, implying a complete loss of energy confinement in this region.

It follows from Eq. (38) that

$$n^{(0)} = \phi^{(0)} + H(\psi). \quad (44)$$

Since  $\phi - n$  is the electron stream-function, the above expression shows that the electron fluid is constrained to flow around magnetic flux-surfaces.

Equations (39) and (41) yield

$$V^{(0)} = \alpha^2 \{F(\phi^{(0)}) - \psi\} \quad (45)$$

and

$$J^{(0)} = - \left( \frac{H' \phi^{(0)} + \alpha^2 (F - \psi)}{\rho^2} \right) - \alpha^2 (1 + \tau)^{-1} \gamma_c H' x + J(\psi). \quad (46)$$

Finally, Eqs. (39) and (40) give

$$0 = [\phi^{(0)}, \rho^2 \phi_{xx}^{(0)} - H + \alpha^2 F'(F - \psi) - \rho^2 \alpha^2 \gamma_c x] + \rho^2 \alpha^2 \tau (1 + \tau)^{-1} \gamma_c [x, H] - \rho^2 \frac{\tau}{2} \{ [\phi_{xx}^{(0)}, n^{(0)}] + [n_{xx}^{(0)}, \phi^{(0)}] + [\phi^{(0)}, n^{(0)}]_{xx} \}. \quad (47)$$

Incidentally, in the above analysis,  $T(\psi)$ ,  $H(\psi)$ ,  $F(\phi^{(0)})$ , and  $J(\psi)$  are, as yet, unknown functions. As we shall see, these functions are determined by *perpendicular transport*.

### C. Expansion in $\rho^2$

Let us now expand  $\phi^{(0)}$  in powers of the small parameter  $\rho^2$ . Thus,

$$\phi^{(0)} = \phi_0 + \rho^2 \phi_1 + O(\rho^4). \quad (48)$$

We shall also assume that  $F - \psi \sim O(\rho^2)$ . To lowest order in  $\rho^2$ , Eq. (47) yields

$$0 = [\phi_0, H(\psi)]. \quad (49)$$

It follows, therefore, that

$$\phi_0 = \phi_0(\psi). \quad (50)$$

Hence, the lowest-order ion stream-function,  $(1 + \tau)\phi_0 + \tau H$ , is a *flux-surface function*. In other words, the ion fluid is also constrained to flow around magnetic flux-surfaces. Incidentally, we can assume that  $\langle \phi_1 \rangle = 0$ , without loss of generality.

Let  $M(\psi) = d\phi_0/d\psi$  and  $L(\psi) = H'(\psi) + M(\psi)$ . The  $y$ -directed ion and electron fluid velocities (in the island rest frame) are directly related to these functions, i.e.,  $V_{yi}/V_* = x(M + \tau L)$  and  $V_{ye}/V_* = x(M - L)$ . Since  $M$  and  $L$  are odd functions of  $x$ , whereas  $\psi$  is an even function, it follows that  $M$  and  $L$  are both constrained to be zero within the magnetic separatrix. In other words, the ion and electron fluids are both *trapped* within the magnetic separatrix, and, thereby, forced to flow at the phase-velocity of the island in this region—see Fig. 8. Note also that, since  $n_x^{(0)} = -xL$ , the density profile is *flattened* within the magnetic separatrix. This implies a complete loss of particle confinement in this region.

Expanding Eq. (47) to next order in  $\rho^2$ , making use of the easily demonstrated results  $F = \psi + \rho^2 \phi_1/M$  and  $F' = 1/M + O(\rho^2)$ , we obtain

$$\phi_1 = \frac{-[M(M + \tau L)/2]' \tilde{x}^2 + \alpha^2 (1 + \tau)^{-1} \gamma_c (M + \tau L) \tilde{x}}{L - M + \alpha^2/M}, \quad (51)$$

where  $\tilde{A} \equiv A - \langle A \rangle / \langle 1 \rangle$ . Finally, expansion of Eq. (46) in  $\rho^2$  yields

$$J^{(0)} = -(L - M + \alpha^2/M) \phi_1 - \alpha^2 (1 + \tau)^{-1} \gamma_c (L - M) \tilde{x} + J(\psi) = [M(M + \tau L)/2]' \tilde{x}^2 - \alpha^2 \gamma_c L \tilde{x} + J(\psi) \quad (52)$$

to lowest order.

### D. First-order terms

Collecting terms that are first-order in our primary ordering scheme, the five-field equations give

$$0 = [\phi^{(1)} - n^{(1)} - \zeta T^{(1)}, \psi] + \rho^4 C J^{(0)}, \quad (53)$$

$$0 = [\phi^{(1)}, n^{(0)}] + [\phi^{(0)}, n^{(1)}] + [V^{(1)} + \rho^2 J^{(1)}, \psi] - \rho^2 \alpha^2 (1 + \tau)^{-1} \gamma_c [x, \phi^{(1)} - n^{(1)}] + \rho^2 D n_{xx}^{(0)}, \quad (54)$$

$$0 = [\phi^{(1)}, \phi_{xx}^{(0)}] + [\phi^{(0)}, \phi_{xx}^{(1)}] + [J^{(1)}, \psi] + \alpha^2 \gamma_c [x, n^{(1)}] - \frac{\tau}{2} \{ [\phi_{xx}^{(1)}, n^{(0)}] + [\phi_{xx}^{(0)}, n^{(1)}] + [n_{xx}^{(1)}, \phi^{(0)}] + [n_{xx}^{(0)}, \phi^{(1)}] + [\phi^{(1)}, n^{(0)}]_{xx} + [\phi^{(0)}, n^{(1)}]_{xx} \} + \rho^2 \mu (\phi^{(0)} + \tau n^{(0)})_{xxxx}, \quad (55)$$

$$0 = [\phi^{(1)}, V^{(0)}] + [\phi^{(0)}, V^{(1)}] + \alpha^2 [n^{(1)} + T^{(1)}/(1 + \tau), \psi] + \rho^2 \chi V_{xx}^{(0)}, \quad (56)$$

$$0 = \rho^{-2} \kappa_{||} [[T^{(1)}, \psi], \psi] + (3/2) [\phi^{(0)}, T^{(0)}] + [V^{(0)} + \zeta \rho^2 J^{(0)}, \psi]. \quad (57)$$

It immediately follows from Eq. (53) that

$$\langle J^{(0)} \rangle = 0. \quad (58)$$

Hence, Eq. (52) reduces to

$$J^{(0)} = [M(M + \tau L)/2]' \tilde{x}^2 - \alpha^2 \gamma_c L \tilde{x}. \quad (59)$$

Now, Eqs. (57) and (53) imply that

$$[T^{(1)}, \psi] \sim O(\rho^4 C), \quad (60)$$

$$[\phi^{(1)} - n^{(1)}, \psi] \sim O(\rho^4 C). \quad (61)$$

So, according to Eq. (56),

$$M[V^{(1)}, \psi] = \alpha^2 [\phi^{(1)}, \psi] + O(\rho^4 \alpha^2 C). \quad (62)$$

Furthermore, it follows from Eq. (55) that  $[J^{(1)}, \psi] \sim O(\rho^2 C)$ . Hence, Eq. (54) gives

$$[\phi^{(1)}, \psi] = [n^{(1)}, \psi] = -\rho^2 D \left( \frac{ML' \tilde{x}^2}{M(L - M) + \alpha^2} \right) + O(\rho^4 C), \quad (63)$$

as well as the solubility condition

$$\langle x^2 \rangle L' - L \langle 1 \rangle \equiv \frac{d}{d\psi} \left( \langle x^2 \rangle \frac{dL}{d\psi} \right) = O(\rho^2). \quad (64)$$

Integrating the above equation, neglecting  $O(\rho^2)$ , and making use of the boundary condition (22), we obtain

$$L(\psi) = \frac{1}{\langle x^2 \rangle} \quad (65)$$

outside the magnetic separatrix.

Finally, the flux-surface average of Eq. (55) yields

$$\begin{aligned} 0 = & \langle [\phi^{(1)}, M' \tilde{x}^2] \rangle + \alpha^2 \gamma_c \langle [x, \phi^{(1)}] \rangle \\ & + \frac{\tau}{2} \{ \langle [n^{(1)}, M' \tilde{x}^2] \rangle + \langle [\phi^{(1)}, L' \tilde{x}^2] \rangle \} \\ & - \frac{\tau}{2} \frac{d}{d\psi} \{ \langle x^2 (L[\phi^{(1)}, \psi] - M[n^{(1)}, \psi]) \rangle \} \\ & + \rho^2 \mu \frac{d^2}{d\psi^2} \{ \langle x^4 \rangle (M' + \tau L') \}. \end{aligned} \quad (66)$$

However,

$$\langle [A, B] \rangle \equiv - \frac{d}{d\psi} \langle \tilde{A}[B, \psi] \rangle, \quad (67)$$

$$\langle x^2 [A, C] \rangle \equiv \frac{d}{d\psi} \langle \tilde{x}^2 [A, C] \rangle, \quad (68)$$

$$\langle [A, x] \rangle \equiv \frac{d}{d\psi} \langle \tilde{x} [A, \psi] \rangle, \quad (69)$$

where  $A, B$  are general fields, but  $C = C(\psi)$ . Thus, Eq. (66) can be integrated to give<sup>18</sup>

$$\begin{aligned} 0 = & \frac{d}{d\psi} \left[ \langle x^4 \rangle \frac{d(M + \tau L)}{d\psi} + \frac{\tau}{2} (D\mu^{-1}) \left( \frac{M(L - M)L'}{M(L - M) + \alpha^2} \right) \langle \tilde{x}^2 \tilde{x}^2 \rangle \right] \\ & - (D\mu^{-1}) \left( \frac{ML'[M' + \tau(L' + M')/2]}{M(L - M) + \alpha^2} \right) \langle \tilde{x}^2 \tilde{x}^2 \rangle \\ & + \gamma_c (D\mu^{-1}) \left( \frac{\alpha^2 ML' \langle \tilde{x} \tilde{x}^2 \rangle}{M(L - M) + \alpha^2} \right) \langle \tilde{x} \tilde{x}^2 \rangle, \end{aligned} \quad (70)$$

where use has been made of the boundary condition (24). The corrections to the above equation are  $O(\rho^2)$ .

Note that  $L(\psi)$  and  $M(\psi)$  are both *discontinuous* on the island separatrix, being zero inside the separatrix, and taking the finite values  $L_{\text{sep}}$  and  $M_{\text{sep}}$ , respectively, just outside the separatrix. In reality, we expect both singularities to be resolved in a separatrix boundary layer of thickness  $O(\rho_s) \ll w$ .<sup>19</sup> According to Eq. (65),  $L_{\text{sep}}$  takes the value  $\pi/4$ . Equation (70) can be solved in a two-stage process. First, assuming that

$$L(\psi) = \frac{\pi}{4} \left[ 1 - \exp\left(\frac{\psi + 1}{\delta}\right) \right] \quad (71)$$

within the separatrix layer, where  $\delta \ll 1$ , we integrate Eq. (70) across the layer, and look for a solution that satisfies  $M(-1) = 0$  and  $M(\psi) \rightarrow M_{\text{sep}}$  as  $(-\psi - 1)/\delta \rightarrow \infty$ . Next, we solve Eq. (70) outside the layer, with  $L(\psi)$  given by Eq. (65),

subject to the boundary conditions  $M(-1) = M_{\text{sep}}$  and  $\sqrt{-2\psi}M \rightarrow -v_\infty$  as  $\psi \rightarrow -\infty$ . The constant  $v_\infty$  determines the island phase-velocity, relative to the equilibrium  $\mathbf{E} \times \mathbf{B}$  velocity,  $V_{EB}$ , via the boundary condition (24), i.e.,

$$V_p = V_{EB} + v_\infty V^*. \quad (72)$$

This procedure uniquely determines the island phase-velocity [since a general solution for  $\sqrt{-2\psi}M(\psi)$  varies like  $\sqrt{-\psi}$  at large  $|\psi|$ , which does not satisfy the large- $|x|$  boundary condition on  $\phi$ ]. (Note that the ion diamagnetic direction is positive, and the electron diamagnetic direction negative, in this paper.) The final result is independent of the details of the boundary layer, provided that  $\delta \ll 1$ , i.e., provided that the boundary layer is much thinner than the island.

Once the function  $M(\psi)$  has been determined, Eqs. (32) and (59) yield the island width evolution equation

$$\frac{dw}{dt} \propto \Delta' \rho_s + \hat{\beta} \rho^3 J_c, \quad (73)$$

where

$$\begin{aligned} J_c = & \left( \frac{32}{3\pi} \right) M_{\text{sep}} (M_{\text{sep}} + \tau L_{\text{sep}}) \\ & + 2 \int_{-1}^{-\infty} \{ [M(M + \tau L)/2]' \langle \tilde{x}^2 \tilde{x}^2 \rangle - \alpha^2 \gamma_c L \langle \tilde{x} \tilde{x}^2 \rangle \} d\psi. \end{aligned} \quad (74)$$

Here, the two terms on the right-hand side of the above equation parametrize the contributions to the free energy available to drive the tearing mode which originate from the boundary layer on the separatrix<sup>20</sup> and the remainder of the inner region,<sup>21</sup> respectively.

## E. Caveat

The above analysis implicitly assumes that the variation length scale in the  $x$  direction is much larger than  $\rho_s$ . Unfortunately, this assumption breaks down in the boundary layer on the separatrix (whose thickness is of order  $\rho_s$ ). The most likely consequence of this breakdown is that the boundary layer will emit *drift-acoustic waves* that propagate to large  $x$ , where they are absorbed by the plasma.<sup>22</sup> If sufficient momentum is carried off by these waves, then the island phase-velocity may be modified from that predicted by the above analysis.

## IV. HYPERSONIC ISLANDS

### A. Introduction

Hypersonic islands are characterized by the secondary ordering  $\alpha \ll 1$  and  $\rho \sim O(1)$ .

### B. Zeroth-order terms

Retaining only zeroth-order terms in our primary ordering scheme, the five-field equations yield Eqs. (38)–(42), which reduce to (see Sec. III B)

$$T^{(0)} = T(\psi), \quad (75)$$

$$n^{(0)} = \phi^{(0)} + H(\psi), \quad (76)$$

$$V^{(0)} = \alpha^2 \{F(\phi^{(0)}) - \psi\}, \quad (77)$$

$$J^{(0)} = -\rho^{-2} \{H' \phi^{(0)} + \alpha^2 F\} - \alpha^2 (1 + \tau)^{-1} \gamma_c H' x + J(\psi), \quad (78)$$

$$0 = [\phi^{(0)}, \rho^2 \phi_{xx}^{(0)} - H - \alpha^2 F' \psi - \rho^2 \alpha^2 \gamma_c x] \\ + \rho^2 \alpha^2 \tau (1 + \tau)^{-1} \gamma_c [x, H] \\ - \rho^2 \frac{\tau}{2} \{[\phi_{xx}^{(0)}, n^{(0)}] + [n_{xx}^{(0)}, \phi^{(0)}] + [\phi^{(0)}, n^{(0)}]_{xx}\}. \quad (79)$$

### C. Expansion in $\alpha^2$

We can expand zeroth-order quantities in the small parameter  $\alpha^2$  by writing

$$T(\psi) = \alpha^2 T_1(\psi), \quad (80)$$

$$H(\psi) = \alpha^2 H_1(\psi), \quad (81)$$

$$\phi^{(0)} = -x + \alpha^2 \phi_1, \quad (82)$$

$$n^{(0)} = -x + \alpha^2 (\phi_1 + H_1), \quad (83)$$

$$F(\phi^{(0)}) = F_0(x) + O(\alpha^2). \quad (84)$$

Equation (78) yields

$$J^{(0)} = \alpha^2 \rho^{-2} (H'_1 \bar{x} - \bar{F}_0) + J(\psi) + O(\alpha^4), \quad (85)$$

whereas Eq. (79) reduces to

$$0 = [x, \rho^2 (1 + \tau) \phi_{1xx} - H_1 + F'_0 \cos \theta] + O(\alpha^2), \quad (86)$$

which can be integrated to give

$$\rho^2 (1 + \tau) \phi_{1xx} = H_1 + K(x) - F'_0 \cos \theta. \quad (87)$$

### D. First-order terms

Retaining only first-order terms in our primary ordering scheme, the five-field equations yield Eqs. (53)–(57).

It immediately follows from Eq. (53) that

$$\langle J^{(0)} \rangle = 0. \quad (88)$$

Hence, Eq. (85) reduces to

$$J^{(0)} = \alpha^2 \rho^{-2} (H'_1 \bar{x} - \bar{F}_0), \quad (89)$$

Equation (57) can be integrated to give

$$[T^{(1)}, \psi] = \alpha^2 \rho^2 \kappa_{\parallel}^{-1} \{-(\zeta H'_1 - (3/2) T'_1) \bar{x} + (\zeta - 1) \bar{F}_0\}, \quad (90)$$

whereas Eq. (53) yields

$$[\phi^{(1)} - n^{(1)}, \psi] = \alpha^2 \rho^2 \{-\{(C + \zeta^2 \kappa_{\parallel}^{-1}) H'_1 - (3/2) \zeta \kappa_{\parallel}^{-1} T'_1\} \bar{x} \\ + [C + \zeta(\zeta - 1) \kappa_{\parallel}^{-1}] \bar{F}_0\}. \quad (91)$$

According to Eq. (56),

$$0 = [V^{(1)}, x] + \alpha^2 \rho^2 \chi (F_0 - \psi)_{xx} + O(\alpha^4 C). \quad (92)$$

It follows that

$$F_{0xx} = \bar{\psi}_{xx} = -1, \quad (93)$$

where  $\bar{\cdot}$  denotes a  $\theta$  average at constant  $x$ . Since  $V$  (and, hence,  $F_0$ ) is an even function of  $x$ , the above equation can be integrated to give

$$F_0 = -\frac{1}{2} x^2. \quad (94)$$

Hence, we conclude that  $V_0 = -\alpha^2 \cos \theta$  and  $V_1 \sim O(\alpha^4 C)$ .

Equation (54) yields

$$0 = [x, \phi^{(1)} - n^{(1)}] + \rho^2 [J^{(1)}, \psi] + \alpha^2 \rho^2 D(H_1 + \phi_1)_{xx} \\ + O(\alpha^4 D), \quad (95)$$

which implies that

$$0 = \langle [x, \phi^{(1)} - n^{(1)}] \rangle + \alpha^2 \rho^2 D \langle (H_1 + \phi_1)_{xx} \rangle. \quad (96)$$

The above equation can be integrated, with the aid of Eq. (67), to give

$$\alpha^2 \langle x^2 \rangle H'_1 + \langle xv \rangle = \rho^{-2} D^{-1} \langle \bar{x} [\phi^{(1)} - n^{(1)}, \psi] \rangle - v_0, \quad (97)$$

where  $v = -\alpha^2 \phi_{1x}$ , and  $v_0$  is a constant.

Finally, Eqs. (54) and (55) yield

$$0 = [(1 + \tau) \rho^2 \phi_{xx}^{(1)} + \phi^{(1)} - n^{(1)}, x] \\ + \alpha^2 \rho^2 \{ \mu(H_1 + K + \tau \rho^2 H_{1xx})_{xx} - D(\phi_1 + H_1)_{xx} \} \\ + O(\alpha^4 C), \quad (98)$$

which reduces to

$$0 = -(D\mu^{-1}) (\overline{\phi_{1xx}} + \overline{H_{1xx}}) + \overline{H_{1xx}} + K_{xx} + \tau \rho^2 \overline{H_{1xxx}}. \quad (99)$$

This equation can be integrated, subject to the boundary conditions (22) and (25), and then combined with Eq. (87), to give<sup>23</sup>

$$\rho^2 \{ (1 + \tau) v + \tau \bar{G} \}_{xx} = (D\mu^{-1}) (\bar{v} + \bar{G}) + (G - \bar{G}) \\ - \alpha^2 \cos \theta, \quad (100)$$

where  $G = \alpha^2 x H'_1$ .

### E. Second-order terms

Retaining only second-order terms in our primary ordering scheme, Eq. (18) yields

$$0 = \rho^{-2} \kappa_{\parallel} \{ [T^{(2)}, \psi], \psi \} + (3/2) [ \phi^{(1)}, T^{(0)} ] + (3/2) [ \phi^{(0)}, T^{(1)} ] \\ + [V^{(1)} + \zeta \rho^2 J^{(1)}, \psi] + \rho^2 \kappa_{\perp} T_{xx}^{(0)}, \quad (101)$$

which can be flux-surface averaged to give

$$(3/2) \langle [x, T^{(1)}] \rangle - \alpha^2 \rho^2 \kappa_{\perp} \langle T_{1xx} \rangle. \quad (102)$$

Integrating the above equation, making use of Eq. (67), and the boundary condition (23), we obtain

$$\langle x^2 \rangle T' = -(3/2) \rho^{-2} \kappa_{\perp}^{-1} \langle \bar{x} [T^{(1)}, \psi] \rangle + \eta_e. \quad (103)$$

Combining the above equation with Eq. (90), we get<sup>14</sup>

$$T' = \frac{\eta_e + (3/2)\alpha^2(\kappa_{\parallel}\kappa_{\perp})^{-1}\{\zeta Y H'_1 + (\zeta - 1)\Xi\}}{\Gamma} \quad (104)$$

outside the separatrix, where

$$Y = \langle \tilde{x}\tilde{x} \rangle, \quad (105)$$

$$\Xi = \frac{1}{2}\langle \tilde{x}\tilde{x}^2 \rangle, \quad (106)$$

$$\Gamma = \langle x^2 \rangle + (3/2)^2(\kappa_{\parallel}\kappa_{\perp})^{-1}Y. \quad (107)$$

Finally, Eqs. (91), (97), and (104) give

$$\alpha^2 H'_1 = - \left\{ \frac{(\langle xv \rangle + v_0)\Gamma + \alpha^2 \Xi \Omega_2 - (3/2)\zeta \eta_e (\kappa_{\parallel} D)^{-1} Y}{\langle x^2 \rangle \Gamma + Y \Omega_1} \right\} \quad (108)$$

outside the separatrix, where

$$G = -|x| \left\{ \frac{(\langle xv \rangle - (1 + \tau)^{-1} \alpha^2 \rho^{-2}/2)\Gamma + \alpha^2 \Xi \Omega_2 - (3/2)\zeta \eta_e (\kappa_{\parallel} D)^{-1} Y}{\langle x^2 \rangle \Gamma + Y \Omega_1} \right\} \quad (113)$$

outside the separatrix, with  $G=0$  inside the separatrix. Note that  $v, G \sim O(\alpha^2) \ll 1$ . It follows that the electron fluid is *trapped* within the magnetic separatrix, while the ion fluid is *largely unaffected* by the island—see Fig. 17. Moreover, the island phase-velocity lies close to the equilibrium electron fluid velocity (since  $V_{ye}/V_*$  is relatively small in the island rest frame). The function  $v(x, \theta)$  satisfies

$$\rho^2 \{(1 + \tau)v + \tau \bar{G}\}_{,xx} = (D\mu^{-1})(\bar{v} + \bar{G}) + (G - \bar{G}) - \alpha^2 \cos \theta. \quad (114)$$

Here,  $Y, \Xi, \Gamma, \Omega_1$ , and  $\Omega_2$  are defined in Eqs. (105)–(107), (109), and (110), respectively. The boundary conditions on  $v$  are

$$v_x = 0 \quad (115)$$

at  $x=0$ , and

$$v \rightarrow v_i + v'_i |x| - (1/2)(1 + \tau)^{-1} \alpha^2 \rho^{-2} x^2 \cos \theta \quad (116)$$

as  $|x| \rightarrow \infty$ . Equations (113)–(116) can be solved via iteration. Incidentally, it follows from Eq. (113) that

$$G \rightarrow -v_i - v'_i |x|, \quad (117)$$

$$n_x = -1 - v - G \rightarrow -1 + (1/2)(1 + \tau)^{-1} \alpha^2 \rho^{-2} x^2 \cos \theta \quad (118)$$

as  $|x| \rightarrow \infty$ .

The perturbed temperature profile  $T(\psi)$  is zero inside the separatrix, and is specified by Eq. (104) outside the separatrix.

$$\Omega_1 = \zeta^2 (\kappa_{\parallel} D)^{-1} \langle x^2 \rangle + (CD^{-1})\Gamma, \quad (109)$$

$$\Omega_2 = \zeta(\zeta - 1)(\kappa_{\parallel} D)^{-1} \langle x^2 \rangle + (CD^{-1})\Gamma. \quad (110)$$

Incidentally, it is easily demonstrated, from self-consistency arguments, that  $v_0 = -(1 + \tau)^{-1} \alpha^2 \rho^{-2}/2$ .<sup>23</sup>

## F. Solution in the inner region

A hypersonic island is characterized by a *flattened* electron temperature profile inside the magnetic separatrix [see Eq. (75)], but a *nonflattened* density profile [see Eq. (83)]. The y-directed electron and ion fluid velocities (in the island rest frame) are written

$$V_{ye}/V_* = -G, \quad (111)$$

$$V_{yi}/V_* = (1 + \tau)(1 + v) + \tau G, \quad (112)$$

respectively. Here,

Finally, the perturbed current in the inner region is given by

$$J^{(0)} = \rho^{-2} \{ \tilde{G} + (1/2)\alpha^2 \tilde{x}^2 \}. \quad (119)$$

Note that

$$J^{(0)} \rightarrow \alpha^2 \rho^{-2} \cos \theta \quad (120)$$

as  $|x| \rightarrow \infty$ . Unfortunately, this implies that the integral  $\int_1^{-\infty} \langle J \cos \theta \rangle d\psi$ , in the island evolution equation (32), is *divergent*. This unphysical behavior can only be prevented if there exists a layer—termed the *intermediate layer*—sandwiched between the inner and outer regions, in which  $J^{(0)}$  decays to zero.<sup>23</sup>

## G. Intermediate layer

The intermediate layer is much wider than the island. It follows that we can *linearize* the five-field equations in this region (since the island is the source of all the nonlinearities in our problem<sup>5</sup>). Let

$$\phi(x, \theta) = -x + \bar{\phi}(x) + \tilde{\phi}(x)e^{i\theta}, \quad (121)$$

$$n(x, \theta) = -x + \bar{n}(x)e^{i\theta}, \quad (122)$$

$$V(x, \theta) = \tilde{V}(x)e^{i\theta}, \quad (123)$$

$$J(x, \theta) = \tilde{J}(x)e^{i\theta}, \quad (124)$$

$$\psi(x, \theta) = -\frac{1}{2}x^2 + e^{i\theta}, \quad (125)$$

where all  $\bar{\phantom{x}}$  and  $\tilde{\phantom{x}}$  terms are first order. It is assumed that  $T = T(\psi)$  in the intermediate layer. The absence of  $\bar{n}(x)$ ,  $\bar{V}(x)$ , and  $\bar{J}(x)$  terms in the above equations is consistent with the behavior of  $n$ ,  $V$ , and  $J$  at the edge of the inner region (see Sec. IV F).

Neglecting transport and curvature terms, linearization of the five-field equations yields

$$(1 + \tau)\rho^2(\tilde{\phi}_{xx} - \bar{v}_{xx}\tilde{\phi}) = (\bar{v} - \alpha^2x^2)\left(\tilde{\phi} - \frac{1}{x}\right) \quad (126)$$

and

$$\tilde{J} = (1 + \tau)\frac{(\tilde{\phi}_{xx} - \bar{v}_{xx}\tilde{\phi})}{x}, \quad (127)$$

where  $\bar{v}(x) = -\bar{\phi}_x(x)$ . Equation (126) is solved subject to the boundary conditions

$$\tilde{\phi} \rightarrow 0 \quad (128)$$

as  $x \rightarrow 0$ , and

$$\tilde{\phi} \rightarrow \frac{1}{x} \quad (129)$$

as  $|x| \rightarrow \infty$ . It follows from Eq. (127) that

$$\tilde{J} \rightarrow 0 \quad (130)$$

as  $|x| \rightarrow \infty$ . Equations (129) and (130) demonstrate that the solution in the intermediate layer can be matched to the conventional ideal-MHD solution (which is  $\tilde{\phi} = 1/x$  and  $\tilde{J} = 0$ ) at very large  $|x|$ .<sup>4,5</sup>

## H. Damping of drift-acoustic waves

Equation (126) is a driven wave equation that describes how electrostatic drift-acoustic waves<sup>9</sup> are excited by the island in the inner region, and then propagate into the intermediate layer.<sup>23</sup> In order to uniquely determine the solution in the layer, we need either to adopt an ‘‘outgoing wave’’ boundary condition at large  $|x|$ ,<sup>24</sup> or to add some form of wave damping to our model. It is more convenient to do the latter. Linearizing Eq. (16), and retaining the perpendicular viscosity, we find that

$$(1 + \tau)\tilde{\phi}_{xx} \rightarrow (1 + \tau)\tilde{\phi}_{xx} + i(1 + \tau)\rho^2\mu\tilde{\phi}_{xxx}. \quad (131)$$

However, it is clear from Eq. (126) that  $(1 + \tau)\rho^2\partial^2/\partial x^2 \rightarrow -\alpha^2x^2$  at large  $|x|$ . This suggests that we should modify Eq. (126) by writing

$$\rho^2(\tilde{\phi}_{xx} - \bar{v}_{xx}\tilde{\phi}) \approx \left(\frac{\bar{v}}{1 + \tau} - \frac{\alpha^2x^2}{1 + \tau - i\alpha^2\mu x^2}\right)\left(\tilde{\phi} - \frac{1}{x}\right), \quad (132)$$

in order to mimic the damping effect of perpendicular viscosity on drift-acoustic waves at large  $|x|$ .

## I. Force balance

The mean  $\mathbf{E} \times \mathbf{B}$  velocity profile in the intermediate layer,  $\bar{v}(x)$ , is determined from *quasilinear force balance*, i.e.,

$$0 = \frac{1}{2}(1 + \tau)\text{Im}(\tilde{\phi}_{xx}\tilde{\phi}^*) - \frac{1}{2}\text{Im}(\tilde{J}) + \rho^2\mu\bar{v}_{xx}. \quad (133)$$

The first term on the right-hand side of the above equation represents the mean Reynolds stress force in the  $y$  direction, the second term the mean  $\mathbf{j} \times \mathbf{B}$  force, and the third term the mean viscous force. Equations (126), (132), and (133) can be combined to give

$$\bar{v}_{xx} = \frac{\rho^{-4}}{2} \frac{(1 + \tau)\alpha^4x^2}{(1 + \tau)^2 + \alpha^4\mu^2x^4} |1 - x\tilde{\phi}|^2. \quad (134)$$

This equation is subject to the boundary conditions

$$\bar{v} \rightarrow v_i + v_i'|x| \quad (135)$$

as  $x \rightarrow 0$ , and

$$\bar{v} \rightarrow -1 - v_\infty \quad (136)$$

as  $|x| \rightarrow \infty$ . Equation (134) describes how momentum carried by drift-acoustic waves radiated by the island is absorbed in the intermediate layer, and modifies the mean velocity profile there.

## J. Solution in the intermediate layer

Our final system of equations in the intermediate layer is

$$\rho^2(\tilde{\phi}_{xx} - \bar{v}_{xx}\tilde{\phi}) = \left(\frac{\bar{v}}{1 + \tau} - \frac{\alpha^2x^2}{1 + \tau - i\alpha^2\mu x^2}\right)\left(\tilde{\phi} - \frac{1}{x}\right) \quad (137)$$

and

$$\bar{v}_{xx} = \frac{\rho^{-4}}{2} \frac{(1 + \tau)\alpha^4x^2}{(1 + \tau)^2 + \alpha^4\mu^2x^4} |1 - x\tilde{\phi}|^2. \quad (138)$$

The boundary conditions are

$$\tilde{\phi} \rightarrow 0, \quad (139)$$

$$\bar{v} \rightarrow v_i + v_i'|x| \quad (140)$$

as  $x \rightarrow 0$ , and

$$\tilde{\phi} \rightarrow \frac{1}{x}, \quad (141)$$

$$\bar{v} \rightarrow -1 - v_\infty \quad (142)$$

as  $|x| \rightarrow \infty$ . The perturbed current is given by

$$\tilde{J} = (1 + \tau)\frac{(\tilde{\phi}_{xx} - \bar{v}_{xx}\tilde{\phi})}{x}. \quad (143)$$

## K. Overall solution

The overall solution to our problem is obtained by generating a solution in the inner region, as described in Sec. IV F, and then finding a matching solution in the intermedi-

ate layer, as described in Sec. IV J. Note that the boundary conditions uniquely specify the overall solution [since a general solution for  $\bar{v}$  increases like  $|x|$  at large  $|x|$ , which does not satisfy the boundary condition (136)].

The island phase-velocity is determined by the constant  $v_\infty$  [see Eq. (142)], i.e.,

$$V_p = V_{EB} + V_* v_\infty. \quad (144)$$

Finally, the island width evolution equation takes the form

$$\frac{dw}{dt} \propto \Delta' \rho_s + \hat{\beta} \rho^3 J_c, \quad (145)$$

where

$$J_c = \int_0^\infty K_c(x) dx, \quad (146)$$

with

$$K_c = \begin{cases} -(2/\pi) \oint \rho^{-2} [\tilde{G} + (1/2)\alpha^2 \tilde{x}^2] \cos \theta d\theta, & x \leq x_c, \\ -2 \operatorname{Re}(\tilde{J}), & x > x_c. \end{cases} \quad (147)$$

Here,  $1 \ll x_c \ll \sqrt{\rho/\alpha}$  is the boundary between the inner region and the intermediate layer.

## V. NUMERICAL RESULTS

### A. Sonic islands

The scheme outlined in Sec. III has been implemented numerically. The aim of the calculation is to determine the island velocity parameter,  $v_\infty$ , and the island stability parameter,  $J_c$ , as functions of the sound-wave parameter,  $\alpha$  [see Eq. (13)], the ion to electron temperature ratio,  $\tau$  [see Eq. (9)], the ratio of transport coefficients,  $D\mu^{-1}$ , and the curvature parameter,  $\gamma_c$  [see Eq. (10)]. The island velocity parameter,  $v_\infty$ , determines the island phase-velocity according to Eq. (72). Thus,  $v_\infty = \tau$  corresponds to an island that propagates with the equilibrium ion fluid,  $v_\infty = 0$ , to an island that propagates with the equilibrium  $\mathbf{E} \times \mathbf{B}$  velocity, and  $v_\infty = -1$  to an island that propagates with the equilibrium electron fluid. The island stability parameter,  $J_c$ , determines the influence of ion polarization currents<sup>21</sup> flowing in the inner region on island stability according to Eq. (73). Thus, if  $J_c > 0$ , then this influence is *destabilizing*, whereas if  $J_c < 0$ , then it is *stabilizing*.

Let us, first of all, consider the zero curvature case,  $\gamma_c = 0$ . Figures 1 and 2 show the island velocity parameter,  $v_\infty$ , as a function of the sound-wave parameter,  $\alpha$  (which is proportional to the island width), for various values of  $\tau$  and  $D\mu^{-1}$ . It can be seen that  $v_\infty \rightarrow \tau$  in the *subsonic* limit  $\alpha \gg 1$ . In other words, wide islands whose widths satisfy  $w \gg \rho_s/\epsilon_n$  propagate with the equilibrium ion fluid.<sup>16</sup> Moreover,  $v_\infty$  becomes less positive as  $\alpha$  is reduced. In other words, narrower islands whose widths satisfy  $w \sim \rho_s/\epsilon_n$  slip somewhat with respect to the unperturbed ion fluid in the *electron* diamagnetic direction.<sup>18</sup> It can also be seen that  $v_\infty \sim 0$  in the *supersonic* limit  $\alpha \ll 1$ . In other words, narrow

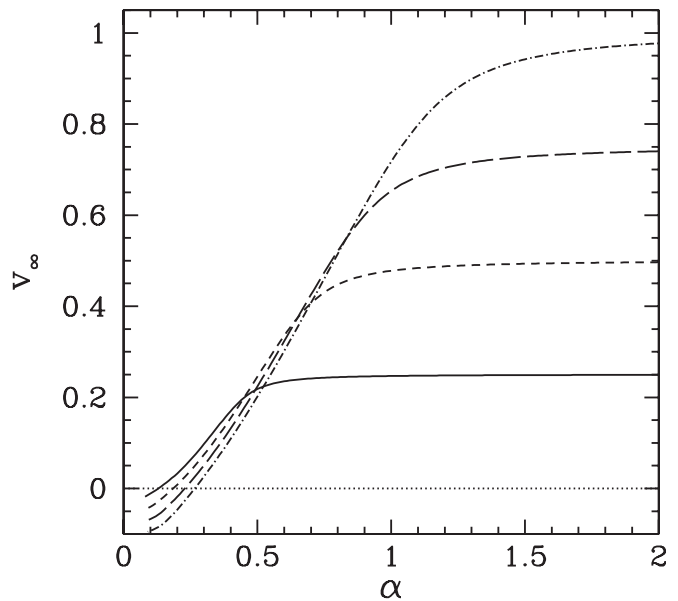


FIG. 1. The island velocity parameter,  $v_\infty$ , as a function of  $\alpha$  for a sonic island with  $D\mu^{-1}=1.0$  and  $\gamma_c=0$ . The solid, short-dashed, long-dashed, and dot-short-dashed curves correspond to  $\tau=0.25, 0.5, 0.75$ , and  $1.0$ , respectively.

islands whose widths satisfy  $\rho_s \ll w \ll \rho_s/\epsilon_n$  propagate close to the unperturbed  $\mathbf{E} \times \mathbf{B}$  velocity. Note, finally, that the transition from the subsonic to the supersonic limits becomes more abrupt as  $D\mu^{-1}$  is reduced.

Figures 3 and 4 show the island stability parameter,  $J_c$ , as a function of the sound-wave parameter,  $\alpha$ , for various values of  $\tau$  and  $D\mu^{-1}$ . It can be seen that  $J_c \rightarrow 0$  both in the *subsonic* limit,  $\alpha \gg 1$ , and the *supersonic limit*,  $\alpha \ll 1$ . It follows that ion polarization currents have a negligible effect on the stability of wide islands whose widths satisfy  $w \gg \rho_s/\epsilon_n$ ,

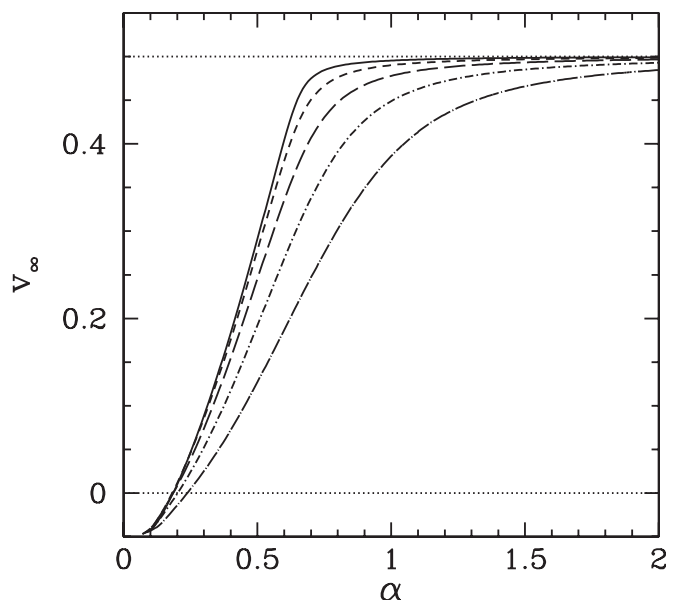


FIG. 2. The island velocity parameter,  $v_\infty$ , as a function of  $\alpha$  for a sonic island with  $\tau=0.5$  and  $\gamma_c=0$ . The solid, short-dashed, long-dashed, dot-short-dashed, and dot-long-dashed curves correspond to  $D\mu^{-1}=0.25, 0.5, 1.0, 2.0$ , and  $4.0$ , respectively.

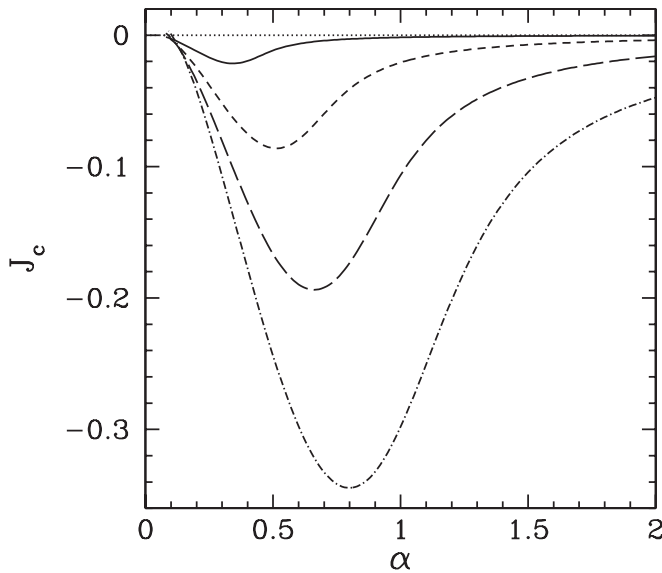


FIG. 3. The island stability parameter,  $J_c$ , as a function of  $\alpha$  for a sonic island with  $D\mu^{-1}=1.0$  and  $\gamma_c=0$ . The solid, short-dashed, long-dashed, and dot-short-dashed curves correspond to  $\tau=0.25, 0.5, 0.75,$  and  $1.0$ , respectively.

or narrow islands whose widths satisfy  $\rho_s \ll w \ll \rho_s / \epsilon_n$ .<sup>25</sup> On the other hand,  $J_c$  peaks at a negative value when  $\alpha \sim 1$ . In other words, ion polarization currents have a stabilizing effect on sonic islands whose widths satisfy  $w \sim \rho_s / \epsilon_n$ .<sup>25</sup> Note that the peak becomes higher as  $\tau$  increases, and narrower (in  $\alpha$ ) as  $D\mu^{-1}$  decreases.

Figure 5 shows the typical ion and electron fluid velocity profiles (in the island rest frame) across the O-point of a sonic island. It can be seen that the island propagates between the equilibrium ion and electron fluid velocities (i.e., the velocities as  $|x| \rightarrow \infty$ ), but is closer to the former. Moreover, the velocity of each fluid increases in magnitude as the

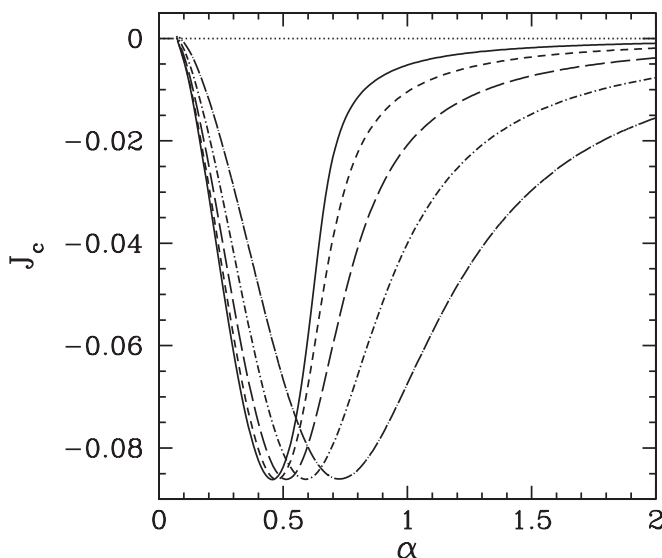


FIG. 4. The island stability parameter,  $J_c$ , as a function of  $\alpha$  for a sonic island with  $\tau=0.5$  and  $\gamma_c=0$ . The solid, short-dashed, long-dashed, dot-short-dashed, and dot-long-dashed curves correspond to  $D\mu^{-1}=0.25, 0.5, 1.0, 2.0,$  and  $4.0$ , respectively.

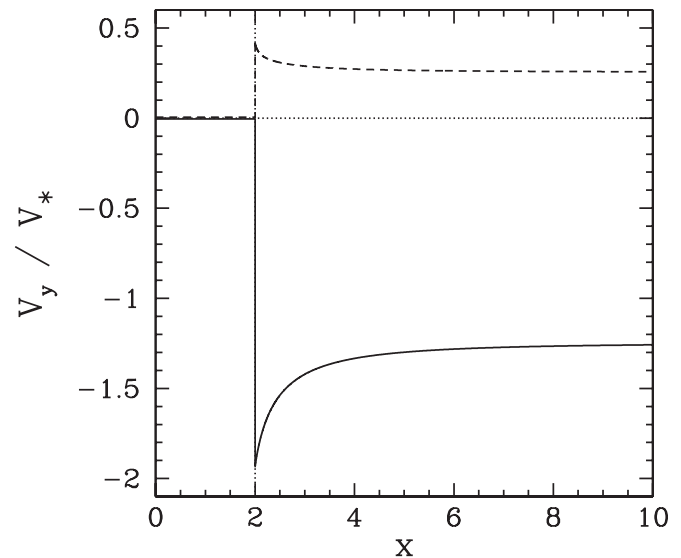


FIG. 5. The  $y$  components of the electron (solid) and ion (dashed) fluid velocities (in the island rest-frame) across the O-point of a sonic island with  $\alpha=0.5, \tau=0.5, D\mu^{-1}=1.0,$  and  $\gamma_c=0$ . The separatrix lies at  $x=2$ .

separatrix is approached from the outside, but is zero inside the separatrix. The velocity discontinuities in both fluids across the separatrix are resolved in a boundary layer (not shown) whose width is of order  $\rho_s$ .

Let us now examine the influence of the average magnetic field-line curvature on sonic islands. It turns out that field-line curvature has a negligible effect on the island phase-velocity. On the other hand, the effect of field-line curvature on island stability is illustrated in Fig. 6. It can be seen that the island is destabilized if  $\gamma_c > 0$  (i.e., if the field-line curvature is unfavorable), and stabilized if  $\gamma_c < 0$ . The influence of field-line curvature on island stability increases

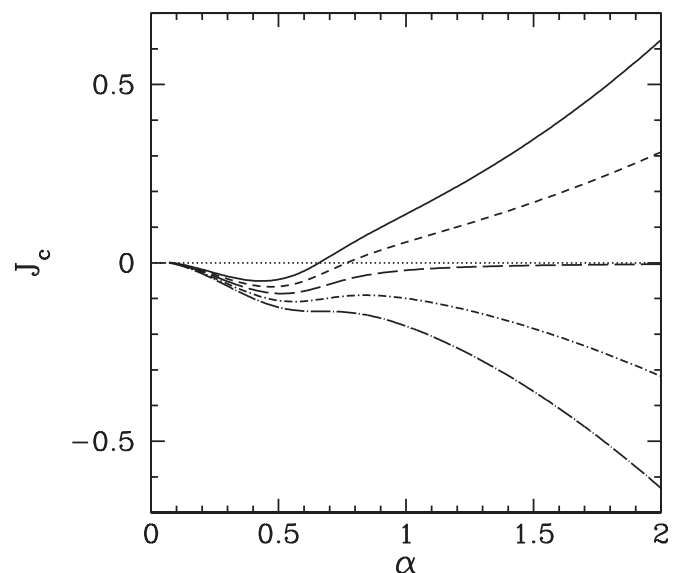


FIG. 6. The island stability parameter,  $J_c$ , as a function of  $\alpha$  for a sonic island with  $\tau=0.5$  and  $D\mu^{-1}=1.0$ . The solid, short-dashed, long-dashed, dot-short-dashed, and dot-long-dashed curves correspond to  $\gamma_c=0.1, 0.05, 0.0, -0.05,$  and  $-0.1$ , respectively.

rapidly with increasing island width, being negligible in the supersonic regime,  $\alpha \ll 1$ , and dominant in the subsonic regime,  $\alpha \gg 1$ .

## B. Hypersonic islands

The scheme outlined in Sec. IV has been implemented numerically. The aim of the calculation is to determine the island velocity parameter,  $v_\infty$  [see Eq. (144)], and the island stability parameter,  $J_c$  [see Eq. (145)], as functions of the remaining free parameters in the model. We can reduce the number of these parameters by observing that  $D \simeq \kappa_\perp$  when  $\beta \ll 1$ , and that  $\kappa_\parallel = 1.63C^{-1}$  according to classical parallel transport theory. Hence,  $(\kappa_\parallel D)^{-1} = (\kappa_\parallel \kappa_\perp)^{-1} = 0.61(CD^{-1})$ . It follows that there are only seven free parameters. These are the normalized island width,  $\hat{w} \equiv \rho^{-1} = w/\rho_s$ , the shear parameter,  $\epsilon_n = L_n/L_s$ , the ion perpendicular viscosity,  $\mu$ , the particle diffusivity,  $D$ , the collisionality,  $CD^{-1}$ , the electron temperature gradient parameter,  $\eta_e = L_n/L_T$ , and the ion to electron temperature ratio,  $\tau = T_i/T_e$ .

Reference 23 examines hypersonic island solutions in the limit of low collisionality—i.e.,  $CD^{-1} = 0$ —and cold ions—i.e.,  $\tau = 0$ . Note, incidentally, that low collisionality hypersonic island solutions have no dependence on  $\eta_e$  [since  $\eta_e$  only appears in our final equations in combination with  $(\kappa_\parallel D)^{-1} \propto CD^{-1}$ ]. The numerically determined dependence of  $v_\infty$  and  $J_c$  on the four remaining free parameters— $\hat{w}$ ,  $\epsilon_n$ ,  $\mu$ , and  $D$ —is

$$v_\infty \simeq -1 + 0.27\hat{w}^3 \epsilon_n^{3/2} D^{-1} + 0.25\hat{w}^4 \epsilon_n^{2/3} \mu^{-4/3} \quad (148)$$

and

$$J_c = -1.5\hat{w}^3 \epsilon_n^{3/2} (1 + 0.25\hat{w}^2 D^{-1}). \quad (149)$$

Moreover, the hypersonic branch of island solutions is found to *cease to exist* above the critical island width

$$\hat{w}_{\max} = 0.9\epsilon_n^{-1/6} D^{1/3}. \quad (150)$$

Recall, incidentally, that  $v_\infty = -1$  corresponds to an island propagating with the equilibrium electron fluid, whereas  $v_\infty = \tau$  corresponds to an island propagating with the equilibrium ion fluid.

According to Eq. (148), a hypersonic island has a phase-velocity that lies between the velocities of the equilibrium ion and electron fluids, but is much closer to the latter. As the island width increases, the deviation of the phase-velocity from the equilibrium electron fluid velocity in the ion diamagnetic direction increases rapidly. Furthermore, according to Eq. (149), a hypersonic island is *stabilized* by ion polarization currents (curvature currents have a negligible effect on hypersonic islands). As the island width increases, this effect also increases rapidly. Finally, it is hypothesized that when the critical island width is exceeded, and the hypersonic solution branch consequently disappears, the island solution bifurcates to the supersonic solution branch.<sup>26</sup> It remains to determine how the above picture is modified in the presence of finite collisionality,  $CD^{-1}$ , finite electron temperature gradient,  $\eta_e$ , and finite ion temperature,  $\tau$ .

Figures 7 and 8 illustrate the influence of finite collisionality, but zero  $\eta_e$  and  $\tau$ , on hypersonic island solutions. In

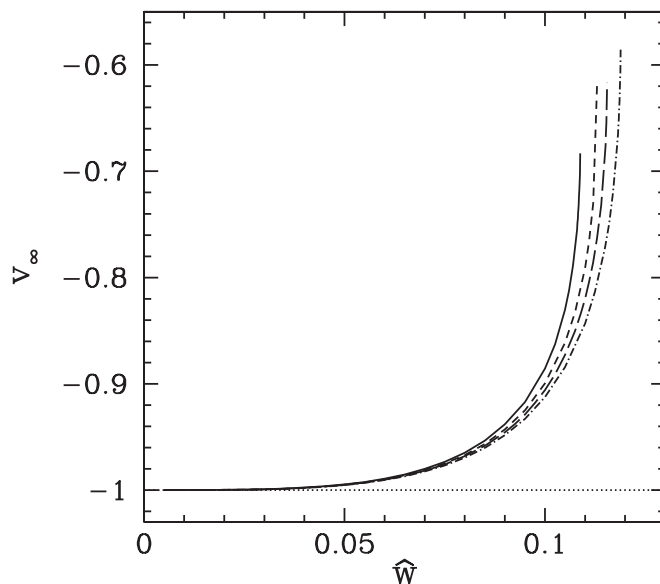


FIG. 7. The island velocity parameter,  $v_\infty$ , as a function of  $\hat{w}$  for a hypersonic island with  $\epsilon_n = 0.1$ ,  $\mu = 10^{-3}$ ,  $D = 5 \times 10^{-4}$ ,  $\eta_e = 0$ , and  $\tau = 0$ . The solid, short-dashed, long-dashed, and dot-short-dashed curves correspond to  $CD^{-1} = 0.0, 1.0, 2.0$ , and  $4.0$ , respectively.

these plots, the island width is increased from zero until the critical island width at which the solution disappears is reached. It can be seen that finite collisionality alone has very little effect on either the phase-velocity or the stability of a hypersonic island.

Figures 9–12 illustrate the effect of finite collisionality and  $\eta_e$ , but zero  $\tau$ , on hypersonic island solutions. It can be seen that the island phase-velocity is *shifted*, relative to that of the standard solution discussed above, in the presence of nonzero  $\eta_e$ . The shift is in the ion diamagnetic direction when  $\eta_e > 0$ , and in the electron diamagnetic direction when  $\eta_e < 0$ , in agreement with Ref. 14. Moreover, the magnitude

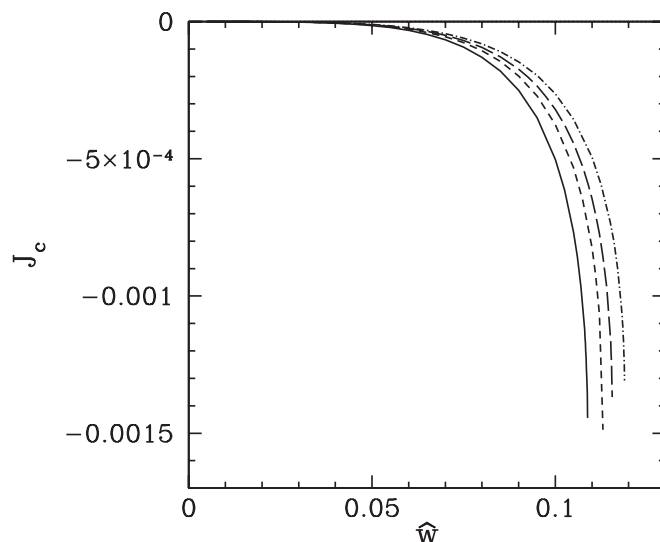


FIG. 8. The island stability parameter,  $J_c$ , as a function of  $\hat{w}$  for a hypersonic island with  $\epsilon_n = 0.1$ ,  $\mu = 10^{-3}$ ,  $D = 5 \times 10^{-4}$ ,  $\eta_e = 0$ , and  $\tau = 0$ . The solid, short-dashed, long-dashed, and dot-short-dashed curves correspond to  $CD^{-1} = 0.0, 1.0, 2.0$ , and  $4.0$ , respectively.

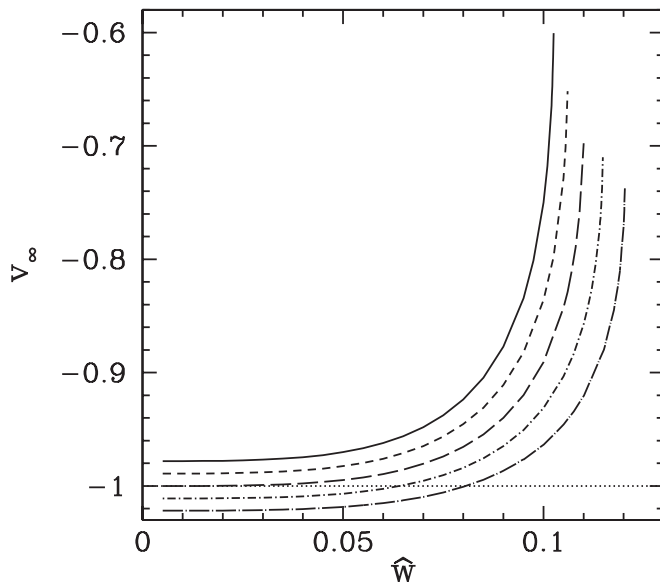


FIG. 9. The island velocity parameter,  $v_\infty$ , as a function of  $\hat{w}$  for a hypersonic island with  $\epsilon_n=0.1$ ,  $\mu=10^{-3}$ ,  $D=5 \times 10^{-4}$ ,  $CD^{-1}=0.25$ , and  $\tau=0$ . The solid, short-dashed, long-dashed, dot-short-dashed, and dot-long-dashed curves correspond to  $\eta_e=1.0, 0.5, 0.0, -0.5$ , and  $-1.0$ , respectively.

of the shift is roughly proportional to the product of the collisionality,  $CD^{-1}$ , and  $|\eta_e|$ . It can also be seen that hypersonic islands that propagate (in the electron diamagnetic direction) faster than the equilibrium electron fluid are *destabilized* by ion polarization currents, whereas those that propagate slower than the equilibrium electron fluid are *stabilized*. It follows that positive  $\eta_e$  is stabilizing (since it tends to make hypersonic islands propagate slower), whereas negative  $\eta_e$  is destabilizing.

Figures 13 and 14 illustrate the effect of finite collisionality and ion temperature, but zero  $\eta_e$ , on hypersonic island

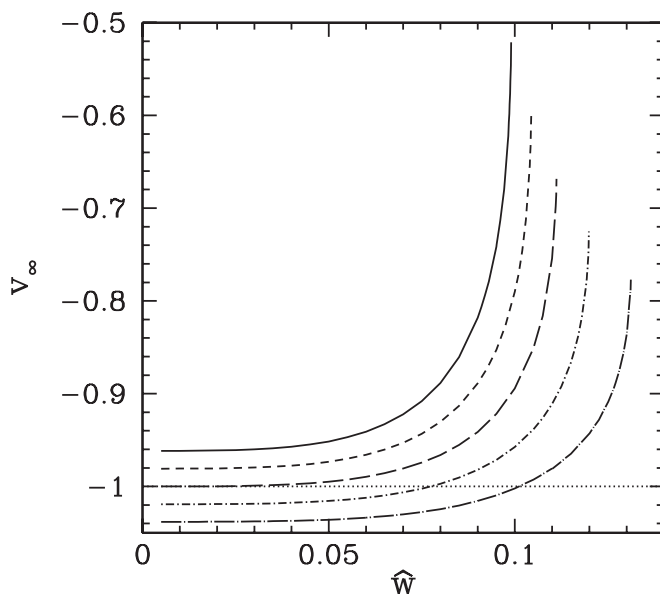


FIG. 10. The island velocity parameter,  $v_\infty$ , as a function of  $\hat{w}$  for a hypersonic island with  $\epsilon_n=0.1$ ,  $\mu=10^{-3}$ ,  $D=5 \times 10^{-4}$ ,  $CD^{-1}=0.50$ , and  $\tau=0$ . The solid, short-dashed, long-dashed, dot-short-dashed, and dot-long-dashed curves correspond to  $\eta_e=1.0, 0.5, 0.0, -0.5$ , and  $-1.0$ , respectively.

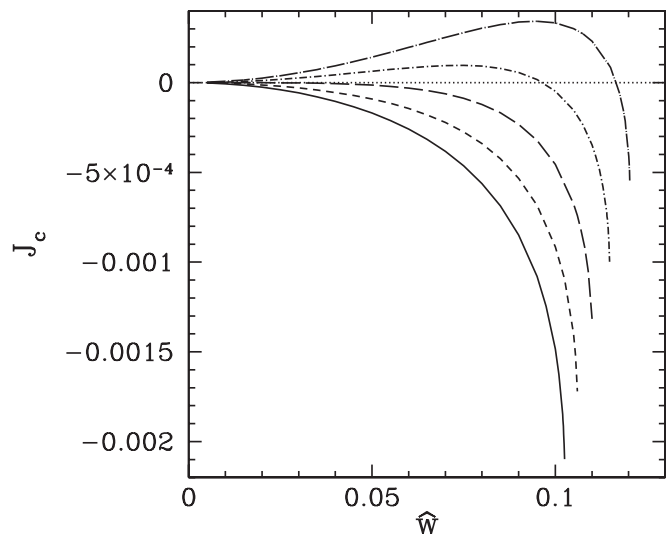


FIG. 11. The island stability parameter,  $J_c$ , as a function of  $\hat{w}$  for a hypersonic island with  $\epsilon_n=0.1$ ,  $\mu=10^{-3}$ ,  $D=5 \times 10^{-4}$ ,  $CD^{-1}=0.25$ , and  $\tau=0$ . The solid, short-dashed, long-dashed, dot-short-dashed, and dot-long-dashed curves correspond to  $\eta_e=1.0, 0.5, 0.0, -0.5$ , and  $-1.0$ , respectively.

solutions. It can be seen that finite ion temperature has comparatively little effect on hypersonic island solutions (apart from a slight modification to the critical island width) when  $\eta_e=0$ .

Figures 15 and 16 illustrate the effect of finite collisionality, ion temperature, and  $\eta_e$ , on hypersonic island solutions. It can be seen that nonzero  $\tau$  gives rise to an additional shift in the island phase-velocity, which decays rapidly as the island width increases. The velocity shift is in the ion diamagnetic direction when  $\eta_e > 0$ , and in the electron diamagnetic direction when  $\eta_e < 0$ . However, the shift seems to have little effect on island stability.

Finally, Fig. 17 shows the typical ion and electron fluid velocity profiles (in the island rest frame) across the O-point

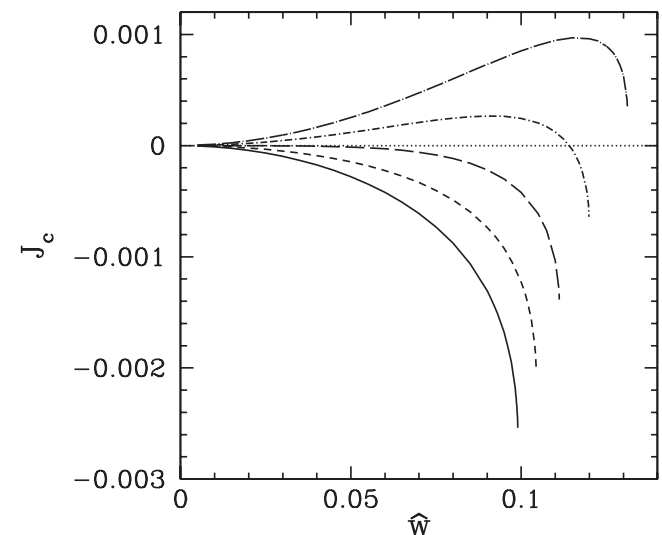


FIG. 12. The island stability parameter,  $J_c$ , as a function of  $\hat{w}$  for a hypersonic island with  $\epsilon_n=0.1$ ,  $\mu=10^{-3}$ ,  $D=5 \times 10^{-4}$ ,  $CD^{-1}=0.5$ , and  $\tau=0$ . The solid, short-dashed, long-dashed, dot-short-dashed, and dot-long-dashed curves correspond to  $\eta_e=1.0, 0.5, 0.0, -0.5$ , and  $-1.0$ , respectively.

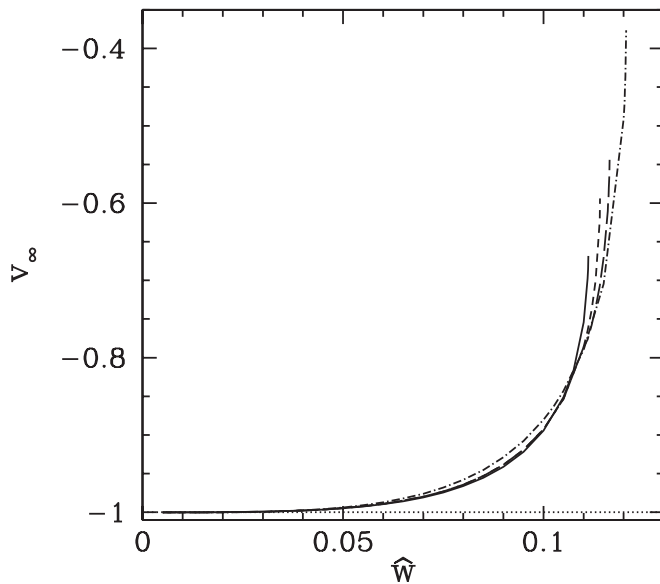


FIG. 13. The island velocity parameter,  $v_\infty$ , as a function of  $\hat{w}$  for a hypersonic island with  $\epsilon_n=0.1$ ,  $\mu=10^{-3}$ ,  $D=5 \times 10^{-4}$ ,  $CD^{-1}=0.5$ , and  $\eta_e=0$ . The solid, short-dashed, long-dashed, and dot-short-dashed curves correspond to  $\tau=0.0, 0.1, 0.2$ , and  $0.5$ , respectively.

of a hypersonic island. It can be seen that the island propagates between the equilibrium ion and electron fluid velocities (i.e., the velocities as  $|x| \rightarrow \infty$ ), but is closer to the latter. Note that the ion fluid velocity profile is essentially unaffected by the island, whereas the electron fluid velocity is constrained to be zero inside the separatrix.

## VI. SUMMARY AND DISCUSSION

We have developed a systematic fluid theory of nonlinear magnetic island dynamics in conventional low- $\beta$ , large aspect-ratio, circular cross-section tokamak plasmas. Our analysis makes use of an extended-MHD model that incor-

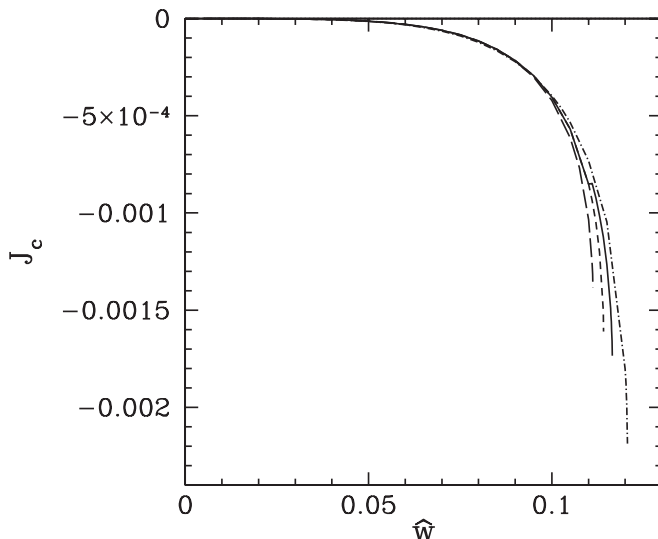


FIG. 14. The island stability parameter,  $J_c$ , as a function of  $\hat{w}$  for a hypersonic island with  $\epsilon_n=0.1$ ,  $\mu=10^{-3}$ ,  $D=5 \times 10^{-4}$ ,  $CD^{-1}=0.5$ , and  $\eta_e=0$ . The solid, short-dashed, long-dashed, and dot-short-dashed curves correspond to  $\tau=0.0, 0.1, 0.2$ , and  $0.4$ , respectively.

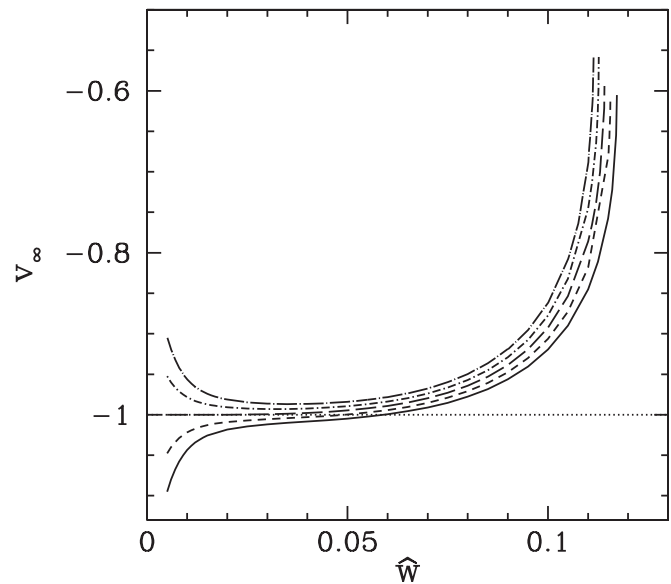


FIG. 15. The island velocity parameter,  $v_\infty$ , as a function of  $\hat{w}$  for a hypersonic island with  $\epsilon_n=0.1$ ,  $\mu=10^{-3}$ ,  $D=5 \times 10^{-4}$ ,  $CD^{-1}=0.5$ , and  $\tau=0.1$ . The solid, short-dashed, long-dashed, dot-short-dashed, and dot-long-dashed curves correspond to  $\eta_e=-0.2, -0.1, 0.0, 0.1$ , and  $0.2$ , respectively.

porates diamagnetic flows, ion gyroviscosity, fast parallel electron heat transport, the ion sound wave, the drift-wave, and average magnetic field-line curvature. The model excludes the compressible Alfvén wave, geodesic field-line curvature, neoclassical effects, and ion Landau damping. Finally, a collisional closure is used for plasma dynamics parallel to the magnetic field.

We have found two distinct branches of island solutions—i.e., the “sonic” and “hypersonic” branches. Both branches are investigated analytically, using suitable ordering schemes, and in each case the problem is reduced to a relatively simple set of nonlinear differential equations that

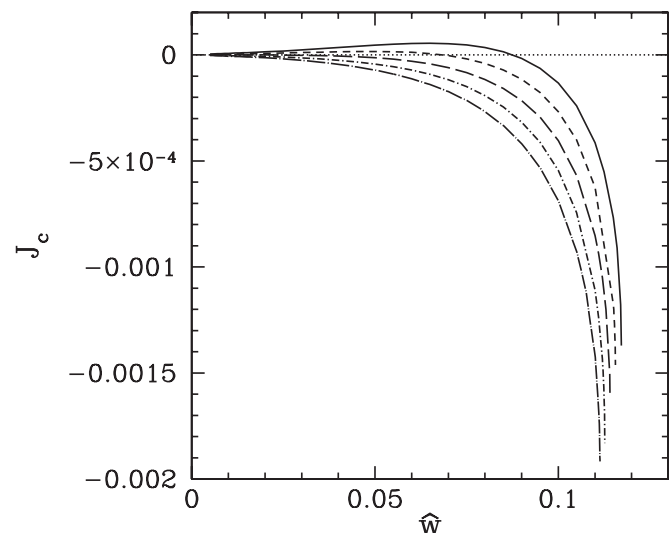


FIG. 16. The island stability parameter,  $J_c$ , as a function of  $\hat{w}$  for a hypersonic island with  $\epsilon_n=0.1$ ,  $\mu=10^{-3}$ ,  $D=5 \times 10^{-4}$ ,  $CD^{-1}=0.5$ , and  $\tau=0.1$ . The solid, short-dashed, long-dashed, dot-short-dashed, and dot-long-dashed curves correspond to  $\eta_e=-0.2, -0.1, 0.0, 0.1$ , and  $0.2$ , respectively.

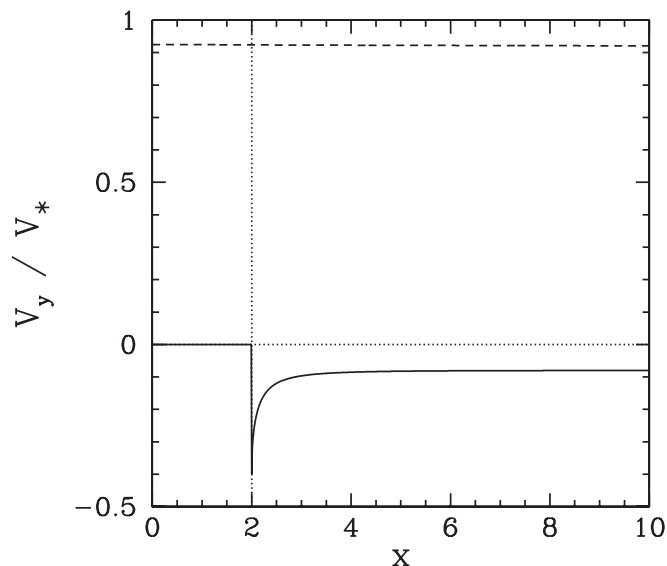


FIG. 17. The  $y$  components of the electron (solid) and ion (dashed) fluid velocities (in the island rest-frame) across the O-point of a hypersonic island with  $\hat{w}=0.09$ ,  $\epsilon_n=0.1$ ,  $\mu=10^{-4}$ ,  $D=5 \times 10^{-3}$ ,  $CD^{-1}=0.5$ ,  $\eta_e=1.0$ , and  $\tau=0$ . The separatrix lies at  $x=2$ .

can be solved numerically via iteration. The solution determines the island phase-velocity, relative to the plasma, and the effect of local currents on the island stability. *Sonic* islands are relatively wide, flatten both the temperature and density profiles, and tend to propagate close to the local ion fluid velocity. *Hypersonic* islands, on the other hand, are relatively narrow, only flatten the temperature profile, radiate drift-acoustic waves, and tend to propagate close to the local electron fluid velocity.<sup>23</sup> The hypersonic solution branch ceases to exist above a critical island width that is of order  $\rho_s$ . Under normal circumstances (i.e.,  $\eta_e > 0$ ,  $L_s > 0$ ), we find that both types of island are *stabilized* by local ion polarization currents.

The fact that there exist two branches of island solutions with very different characteristics was first established via numerical simulation by Ottaviani *et al.*<sup>26</sup> These researchers also found that the hypersonic branch ceases to exist above a critical island width, whereas the sonic branch ceases to exist below a somewhat smaller critical island width, and that the disappearance of a given solution branch triggers a bifurcation to the other branch. Our analysis confirms that the hypersonic solution branch ceases to exist above a certain critical island width. Unfortunately, our ordering scheme precludes us from extending the sonic solution branch to small island widths (i.e.,  $w \sim \rho_s$ ), so we cannot confirm that this branch ceases to exist below some critical width. Clearly, more work is needed in this area.

The analysis presented in this paper builds on analysis previously presented in Refs. 12, 14, 15, 18, 23, and 19 and

will, hopefully, form the foundations of a fully comprehensive fluid theory of nonlinear magnetic island dynamics in low- $\beta$ , large aspect-ratio, circular cross-section tokamak plasmas. Ideally, this theory will incorporate neoclassical effects, such as the bootstrap current<sup>27</sup> and ion poloidal flow damping,<sup>28</sup> will not employ a collisional closure for parallel dynamics,<sup>29</sup> and will take geodesic magnetic field-line curvature into account.<sup>30</sup> The ultimate goal of such a theory is to predict the stability of neoclassical tearing modes<sup>31</sup> in ITER.<sup>32</sup>

## ACKNOWLEDGMENTS

This research was funded by the U.S. Department of Energy under Contract No. DE-FG05-96ER-54346.

- <sup>1</sup>J. A. Wesson, *Tokamaks*, 3rd ed. (Oxford University Press, Oxford, 2004).
- <sup>2</sup>J. P. Freidberg, *Ideal Magnetohydrodynamics* (Springer, Berlin, 1987).
- <sup>3</sup>J. A. Wesson, Nucl. Fusion **18**, 87 (1978).
- <sup>4</sup>H. P. Furth, J. Killeen, and M. N. Rosenbluth, Phys. Fluids **6**, 459 (1963).
- <sup>5</sup>P. H. Rutherford, Phys. Fluids **16**, 1903 (1973).
- <sup>6</sup>F. Militello and F. Porcelli, Phys. Plasmas **11**, L13 (2004).
- <sup>7</sup>D. F. Escande and M. Ottaviani, Phys. Lett. A **323**, 278 (2004).
- <sup>8</sup>Z. Chang and J. D. Callen, Nucl. Fusion **30**, 219 (1990).
- <sup>9</sup>R. D. Hazeltine and J. D. Meiss, *Plasma Confinement* (Dover, New York, 2003).
- <sup>10</sup>A. Zeiler, J. F. Drake, and B. Rogers, Phys. Plasmas **4**, 2134 (1997).
- <sup>11</sup>D. Grasso, M. Ottaviani, and F. Porcelli, Nucl. Fusion **42**, 1067 (2002).
- <sup>12</sup>F. L. Waelbroeck, Phys. Rev. Lett. **95**, 035002 (2005).
- <sup>13</sup>R. D. Hazeltine, M. Kotschenreuther, and P. J. Morrison, Phys. Fluids **28**, 2466 (1985).
- <sup>14</sup>F. Waelbroeck, Plasma Phys. Controlled Fusion **49**, 905 (2007).
- <sup>15</sup>M. Kotschenreuther, R. D. Hazeltine, and P. J. Morrison, Phys. Fluids **28**, 294 (1985).
- <sup>16</sup>R. Fitzpatrick and F. L. Waelbroeck, Phys. Plasmas **12**, 022307 (2005).
- <sup>17</sup>B. D. Scott, A. B. Hassam, and J. F. Drake, Phys. Fluids **28**, 275 (1985).
- <sup>18</sup>R. Fitzpatrick, P. G. Watson, and F. L. Waelbroeck, Phys. Plasmas **12**, 082510 (2005).
- <sup>19</sup>J. W. Connor, F. L. Waelbroeck, and H. R. Wilson, Phys. Plasmas **8**, 2835 (2001).
- <sup>20</sup>F. L. Waelbroeck and R. Fitzpatrick, Phys. Rev. Lett. **78**, 1703 (1997).
- <sup>21</sup>A. I. Smolyakov, Plasma Phys. Controlled Fusion **35**, 657 (1993).
- <sup>22</sup>R. Fitzpatrick and F. L. Waelbroeck, Phys. Plasmas **12**, 122511 (2005).
- <sup>23</sup>R. Fitzpatrick and F. L. Waelbroeck, Phys. Plasmas **14**, 122502 (2007).
- <sup>24</sup>L. D. Perlstein and H. L. Berk, Phys. Rev. Lett. **23**, 220 (1969).
- <sup>25</sup>R. Fitzpatrick, F. Militello, and F. L. Waelbroeck, Phys. Plasmas **13**, 122507 (2006).
- <sup>26</sup>M. Ottaviani, F. Porcelli, and D. Grasso, Phys. Rev. Lett. **93**, 075001 (2004).
- <sup>27</sup>R. Carrera, R. D. Hazeltine, and M. Kotschenreuther, Phys. Fluids **29**, 899 (1986).
- <sup>28</sup>T. H. Stix, Phys. Fluids **16**, 1260 (1972).
- <sup>29</sup>R. D. Hazeltine and S. M. Mahajan, Phys. Plasmas **9**, 3341 (2002).
- <sup>30</sup>A. I. Smolyakov, X. Garbet, and M. Ottaviani, Phys. Rev. Lett. **99**, 055002 (2007).
- <sup>31</sup>O. Sauter, R. J. La Haye, Z. Chang, D. A. Gates, Y. Kamada, H. Zohm, A. Bondeson, D. Boucher, J. D. Callen, M. S. Chu, T. A. Gianakon, O. Gruber, R. W. Harvey, C. C. Hegna, L. L. Lao, D. A. Monticello, F. Perkins, A. Pletzer, A. H. Reiman, M. Rosenbluth, E. J. Strait, T. S. Taylor, A. D. Turnbull, F. Waelbroeck, J. C. Wesley, H. R. Wilson, and R. Yoshino, Phys. Plasmas **4**, 1654 (1997).
- <sup>32</sup>Y. Shimomura, Fusion Eng. Des. **55**, 97 (2001).